Local mechanical behaviour of structural sandwich elements at an intermediate support

R.A. Luimes

Eindhoven University of Technology, Eindhoven, the Netherlands

A.J.M. Jorissen

Eindhoven University of Technology, Eindhoven, the Netherlands

Structural sandwich elements composed of chipboard facings and an EPS core are ideal for application in roof structures. The advantageous properties of chipboard and EPS are used to strive for optimum use of materials, low dead weight, high strength and high thermal insulation capacity. As a consequence, structural sandwich elements are sensitive for local brittle bending tensile failure of the inside of the lower facing at an intermediate support. In this research, an analytical, experimental and numerical analysis of the local mechanical behaviour of structural sandwich elements at an intermediate support is performed. An improved and reliable analytical design approach for this local mechanical behaviour is determined and proposed to be used in practice.

Key words: Sandwich element, EPS, chipboard, local behaviour, brittle bending tensile failure

1   Introduction

A sandwich element is generally composed of two facings and a core, as shown in Figure 1. The facings are relatively thin and have a high strength, whereas the core is relatively thick and light having adequate stiffness to support the facings in the direction perpendicular to the facings. Sandwich elements can be composed of many different combinations of materials. Facings can be made of steel, aluminium, wood, fibre-reinforced plastic or concrete and cores can be made of solid plastic material (polyethylene), rigid foam material (polyurethane or polystyrene) or honeycombs of paper or steel. The various combinations of materials that form sandwich elements allow for optimum solutions to specific applications.

Figure 1. Composition of a typical sandwich element

The research described in this paper focuses on the combination of chipboard facings and an expanded polystyrene core (EPS) (Fig. 2). These types of structural sandwich elements combine the advantageous properties of chipboard, having load-bearing capacity and the ability to protect the core from mechanical damage and fire with those of EPS being light-weight and providing thermal and acoustic insulation. Both materials are bonded together with an adhesive and perform as a composite structure resulting in structural sandwich elements that are ideal for application in wall- and roof structures (Fig. 3).
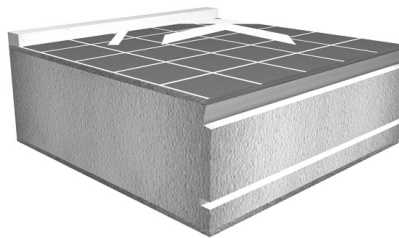

Figure 2. Structural sandwich element composed of chipboard facings and an expanded polystyrene (EPS) core [10]

Figure 3. Structural sandwich roof element that is hoisted onto a precast concrete floor [10]

Structural sandwich roof elements are an innovative solution for the efficient and fast construction of roof structures. The advantageous properties of chipboard and EPS can be used to strive for structural sandwich roof elements that achieve the optimum use of materials, low dead weight, high strength, large spans and high thermal insulation capacity. As a consequence of this pursuit, structural sandwich roof elements are sensitive to facing, core and adhesive stresses which can induce local failure.

Analytical solutions concerning local mechanical behaviour of structural sandwich elements are derived by Stichting Keuringsbureau Hout (SKH) [1] and Davies [2]. Both publications describe univocal local mechanical behaviour. However, both publications are not univocal regarding the derivation and formulation of the analytical solutions. Moreover, experimental analysis performed by De Groot [3] indicates that the analytical solutions may lead to unsafe situations as the ultimate failure load is overestimated.

The problem definition of this research is therefore formulated as follows:
- Existing analytical solutions that describe local mechanical behaviour of structural sandwich elements at an intermediate support are not univocal.
- Existing analytical solutions that describe the local mechanical behaviour of structural sandwich elements at an intermediate support may be unsafe as the ultimate failure load is overestimated.

Performing research is essential to obtain more insight in the local mechanical behaviour of structural sandwich elements leading to improved and reliable analytical solutions to prevent possible unsafe situations in practice. The gathered increased understanding of the local mechanical behaviour will not only result in improved analytical solutions, but may also contribute to an optimal design of the structural sandwich element.

The objective of the research project is therefore formulated as follows:

The research objective is to formulate an improved and reliable analytical design approach of the local mechanical behaviour of structural sandwich elements at an intermediate support.

In addition to the research objective, several assumptions, simplifications and limitations are made to narrow down the scope of this research project. The following general assumptions, simplifications and limitations are made.

- Structural sandwich element type Unidek Kolibrie 3.5 [10]; this type of structural sandwich roof element is considered in all analyses of the research project, because it is most prone to local failure due to the relative small thickness of the facings.

- Global mechanical behaviour; the global mechanical behaviour of structural sandwich elements that span three or more supports (statically undetermined) can be described by the formulas derived by Berner [4] and De Groot [3]. These formulas are adopted in this research.

- Analysis of local mechanical behaviour; this research project is limited to the analysis of the local mechanical behaviour at an intermediate support of a two-span structural sandwich roof element with equal spans. Brittle bending tensile failure of the inside of facing 2 (Fig. 1) is assumed to be the governing failure mechanism. Other theoretically possible local failure mechanisms, like shear failure of the facing, crushing failure of the core and tensile failure of the adhesive are not considered.

- Adhesive layer; the influence of the adhesive layer between the facings and the core is not taken into account. The influence of the bending and shear stiffness of the adhesive layer is neglected and it is assumed that the facings and the core behave as a composite structure. Furthermore, tensile or shear failure of the adhesive layer are not considered.

- Two-dimensional problem; a structural sandwich roof element spans in one direction (first direction) and is assumed to deform only in the direction normal to the plane (second direction), therefore a plane stress state in the direction along the plane (third direction) is assumed and the analysis of the local behaviour can be modelled as a two-dimensional problem.

In chapter 2, an outline of the local mechanical behaviour and failure mechanism of structural sandwich elements at an intermediate support is given. In chapter 3, an analytical analysis of the local mechanical behaviour is outlined by presenting an analysis approach. Analytical limit states and corresponding analytical solutions concerning the local mechanical behaviour and failure of the lower facing and core are discussed. Subsequently, chapter 3 and 4 outline an experimental and numerical analysis of the local mechanical behaviour. The results of the analytical, experimental and numerical analysis are compared and discussed. Finally, chapter 5 outlines the conclusions.

2   Local mechanical behaviour

In this chapter, the local mechanical behaviour of a structural sandwich element at an
intermediate support is outlined. In general, the externally applied load on structural
sandwich roof elements can be represented by a uniformly distributed load (Fig. 4a). A
two-span structural sandwich element subjected to a uniformly distributed load develops a
negative bending moment and a reaction force at the intermediate support. It is assumed
that the two facings carry the negative bending moment as a combination of tensile and
compressive reaction forces since the bending stiffness of the core is low (Fig. 4b). The
lower facing of the sandwich element is then subjected to an in-plane compressive load
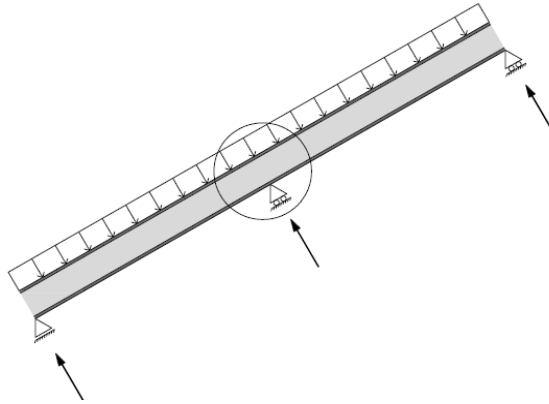and an out-of-plane load (Fig. 4c).

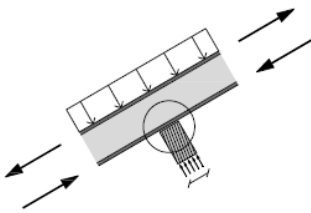*Figure 4a. A two-span structural sandwich roof element*

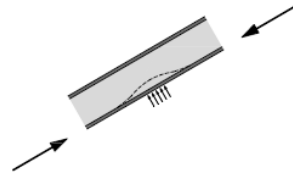*Figure 4b. Loads at the intermediate support*   *Figure 4c. Loads imposed on the lower facing*

The in-plane compressive load N imposed on the lower facing causes an uniform in-plane
pure compressive stress $\sigma_{c,pure}$ over the thickness of the facing (Fig. 5b). The out-of-plane
load F imposed on the lower facing causes an out-of-plane deformation of the lower facing.
The in-plane compressive load imposed on the deformed lower facing causes an additional
deformation of the lower facing until equilibrium (stable situation) is reached. The

deformation of the lower facing induces a bending moment in the lower facing resulting in bending stress over the thickness of the lower facing (Fig. 5b). The bending stress σ_m varies from compression $\sigma_{m;c}$ to tension $\sigma_{m;t}$ over the thickness of the lower facing and along the length of the lower facing. The maximum facing bending stress σ_m can be found at the location of maximum deformation, point (A) (Fig. 5a).
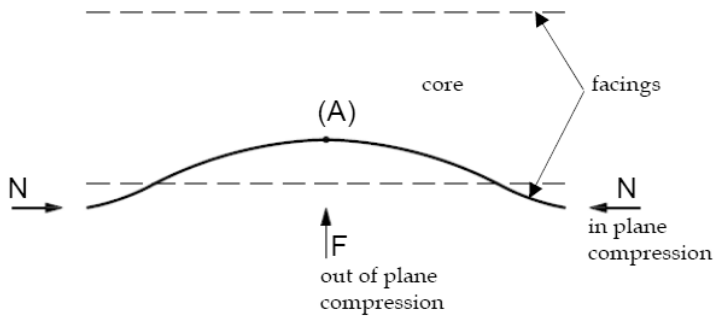

Figure 5a. Out-of-plane deformation of the lower facing

$\sigma_{c,tot}$ = total compresive stress
$\sigma_{c,pure}$ = pure compressive stress
σ_t = tensile stress
$\sigma_{m,c}$ = bending compressive stress
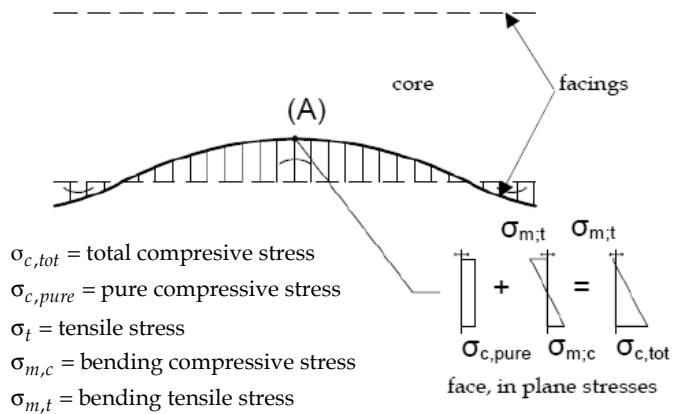$\sigma_{m,t}$ = bending tensile stress

Figure 5b. In-plane compressive and bending stress in de lower facing
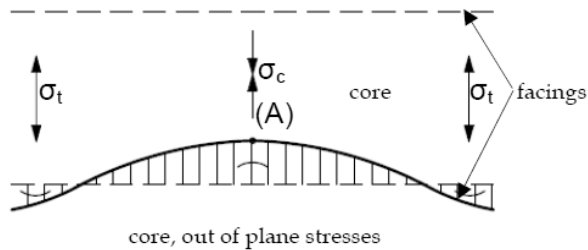

Figure 5c. Out-of-plane compressive and tensile stress in the core

In point (A), the maximum total facing compressive stress $\sigma_{c,tot}$ can be found at the outside of the lower facing and is composed of a component due to pure compression $\sigma_{c,pure}$ and a component due to bending $\sigma_{m;c}$ (Fig. 5b). Bending tensile stress $\sigma_{m;t}$ can be found at the interface of the lower facing and the core, inside of the lower facing, if the bending tensile stress $\sigma_{m;t}$ exceeds the pure compressive stress $\sigma_{c,pure}$. If the bending tensile stress $\sigma_{m;t}$ increases, this will finally induce brittle bending tensile failure of the inside of the lower facing.

The out-of-plane deformation of the facing is resisted by the core. This resistance causes compressive stress σ_c and tensile stress σ_t in the core in the direction normal to the facing plane (Fig. 5c). The maximum core compressive stress can be found at the interface of the lower facing and the core and at the location of maximum deformation, point A.

3   Analytical analysis

In this chapter, an analytical analysis of the, in chapter 2 outlined, local mechanical behaviour of a structural sandwich element at an intermediate support is discussed. As already outlined in the introduction, publications by SKH [1] and Davies [2] provide analytical solutions concerning this local mechanical behaviour. The publication by Davies [2] provides a more extensive description of the local mechanical behaviour and is therefore adapted in this research.

3.1   Analysis Approach

The local mechanical behaviour of structural sandwich elements at an intermediate support is idealized and simplified such that the local mechanical behaviour of the lower facing and the core can be determined analytically and limit states for both the facing and core can be presented. The analytical approach to determine the limit states is illustrated in Figure 6. The first step of the analytical approach consists of determining a proper mechanical model that represents the structural sandwich element at an intermediate support (step 1a) and determining the material and mechanical properties (step 1b). The second step consists of the choice of a foundation constant (step 2a) and the choice of the model that accurately takes into account the influence of the out-of-plane load (step 2b). Finally, limit states for both the facing and core can be determined (step 3).
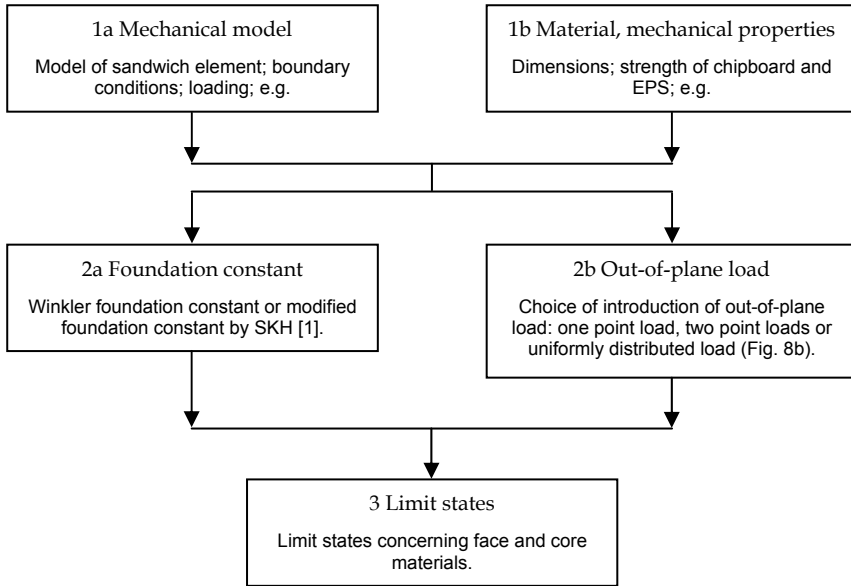
Figure 6. Flow chart representing the analysis approach to analytically determine the local mechanical behaviour of the lower facing and the core of structural sandwich elements at an intermediate support

3.1.1 Mechanical model (step 1a)

The local mechanical behaviour outlined in chapter 2 (Fig. 5a) can be modelled by a beam on a continuous elastic foundation subjected to an in-plane compressive load N and an out-of-plane load F in which the lower facing is represented by the beam and the core is represented by the continuous elastic foundation (Fig. 7-left).

The theory of Winkler is adopted to analytically describe the behaviour of the core. The continuous elastic foundation that represents the core is therefore simplified into a Winkler foundation as it is difficult to evaluate the complex behaviour of a continuous elastic medium analytically. A Winkler foundation is regarded the simplest form to mathematically represent an elastic medium. In a Winkler foundation there is no continuity in the elastic material. Therefore, it can be represented by a series of independent springs that are placed infinitesimally close together [5] (Fig. 7-right).
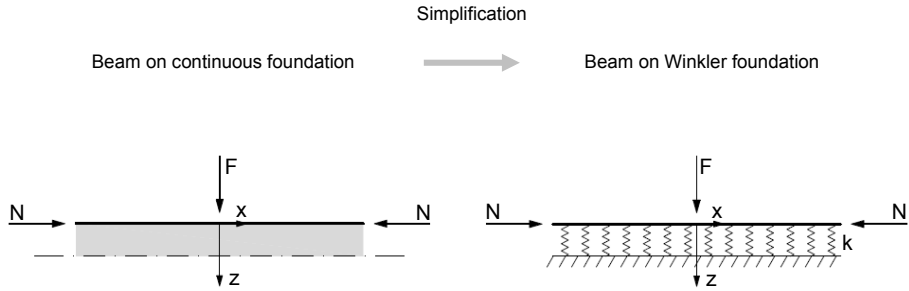
150

Simplification

Beam on continuous foundation → Beam on Winkler foundation

Figure 7. A beam on a continuous foundation (left) can be simplified into a beam on a Winkler foundation (right)

3.1.2 Material and mechanical properties (step 1b)

The material and mechanical properties of the facings, chipboard P5 produced by Wilhelm Mende GmbH & Co, and the core, EPS type 60 produced by Kingspan - Unidek B.V., need to be established accurately as they can have a significant influence on the local mechanical behaviour.

In this research the values of the mechanical properties as presented in Table 1 and 2 of chipboard P5 and EPS type 60 published by De Groot [3] are adopted. Missing values are taken from, Blaß et al [6] and EOTA [7] (Table 1 and 2).

In this research the material dimensions of sandwich element type Unidek Kolibrie 3.5 [10] are adopted. The thickness of the chipboard P5 is set to 3 mm and the thickness of the EPS type 60 is set to 137 mm.

3.1.3 Foundation constant (step 2a)

As outlined in paragraph 3.1.1 the mechanical model to represent the local mechanical behaviour consists of a beam on a Winkler foundation. The foundation constant of a Winkler foundation can be defined as [5]:

$$k = \frac{E_{c;c}}{h} \ ,$$

(1)

where, $E_{c;c}$ is the modulus of elasticity in compression of the core and h is the core thickness. A more complex foundation constant is presented by the SKH publication [1] according to Eq. 2, based on experimental results (curve fitting).

$$k = 0.27 E_{c;c} \sqrt[3]{\dfrac{E_{c;c}}{E_{f;m} I_f}} \ , \tag{2}$$

where, $E_{f;m} I_f$ is the bending stiffness of the facing.

Table1. Mechanical properties of chipboard according to Blaß et al [6], EOTA [7] and De Groot [3]. The grey coloured values are not adopted in this research.

Chipboard P5			Blaß et al [6]	EOTA [7]	De Groot [3]	
In-plane	$f_{f;m;k}$	N/mm²	9.4			
	$f_{f;c;k}$	N/mm²	*12.7*	*12.0*	14.38	
	$f_{f;t;k}$	N/mm²	*9.4*	*8.9*	6.24	
	$E_{f;m}$	N/mm²	2000	*1800*		
	$E_{f;c}$	N/mm²	*2000*	*1800*	3183	
	$E_{f;t}$	N/mm²	*2000*	*1800*	3397	
	G_f	N/mm²	960	*860*		
Out-of- plane	$f_{f;m;k}$	N/mm²	*15.0*		16.06*	22.68**
	$f_{f;c;k}$	N/mm²	10.0			
	$f_{f;t;k}$	N/mm²				
	$E_{f;m}$	N/mm²	*3500*	*3200*	3713*	3860**
	$E_{f;c}$	N/mm²	3500	*3200*		
	$E_{f;t}$	N/mm²	3500	*3200*		
	G_f	N/mm²	200	200		

*One side of chipboard P5 is equipped with a thin foil. The bending modulus of elasticity and bending strength are determined by a bending test in which the foil is subjected to compression.
**One side of chipboard P5 is equipped with a thin foil. The bending modulus of elasticity and bending strength are determined by a bending test in which the foil is subjected to tension.

Table 2. Mechanical properties of EPS according to the EOTA [7] and De Groot [3]. The grey coloured value is not adopted in this research.

EPS60			EOTA [7]	De Groot [3]
	$f_{c;c;k}$	N/mm²	0.060	
	$f_{c;t;k}$	N/mm²	0.100	
	$f_{c;v;k}$	N/mm²	0.050	
	$E_{c;c}$	N/mm²	4	
	G_c	N/mm²	*1.82*	1.84

This foundation constant is derived by comparing the behaviour of a beam on a continuous foundation and a beam on a Winkler foundation. The application of this complex foundation constant in the Winkler theory results in more accurate analytical solutions. Therefore, the foundation constant presented by the SKH publication [1] is adopted in this research.

3.1.4 Introduction out-of-plane load (step 2b)

As outlined in chapter 2, a two-span structural sandwich roof element subjected to an uniformly distributed load develops a reaction force at the intermediate support. The reaction force is in the mechanical model (Fig. 7) represented by the out-of-plane load F. According to Davies [2], the reaction force and thus out-of-plane load F can be introduced in three different ways: one point load, two point loads or a uniformly distributed load, as is illustrated in Figure 8. The introduction of the out-of-plane load as two point loads, two times F/2 as indicated in Figure 8b, is considered most realistic in practice, as due to an increasing externally applied load the sandwich element will curve over the width of the support and will finally rest on the edges of the support (Fig. 8c).
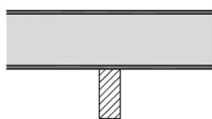

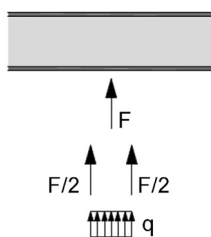Figure 8a. Structural sandwich element at an intermediate support

Figure 8b. The introduction of out-of-plane load can be modelled by one point load, two point loads or a uniformly distributed load
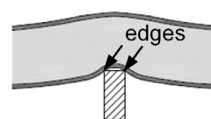
Figure 8c. Structural sandwich element resting on the edges of the intermediate support

3.1.5 Limit states (step 3)

The local mechanical behaviour outlined in chapter 2, can be described analytically by the limit states and corresponding analytical solutions (paragraph 3.2) by Davies [2]. In chapter 2, the governing failure mechanism is defined as brittle bending tensile failure of the inside of the lower facing (Fig. 5b). This failure mechanism occurs due to the fact that both the outside of the lower facing and the core show physical non-linear behaviour.

Davies [2] distinguishes three limit states for the local mechanical behaviour; two for the lower facing and one for the core. As these limit states are only valid for physical linear and geometrical non-linear behaviour, physical non-linear behaviour of the outside of the lower facing and the core and thus brittle bending tensile failure is not captured.

The facing compressive stress is limited by the critical facing (buckling) stress.

$$\sigma_{f;c;x} \leq \sigma_{cr} \tag{3}$$

where, x is the in-plane direction. The critical facing stress is given by Allen [8]. A derivation of the critical facing (buckling) stress is also given in [9].

$$\sigma_{cr} = 0.78 \sqrt[3]{E_{f;m} E_{c;c} G_c} \tag{4}$$

where, $E_{f;m}$ is the modulus of elasticity in bending of the facing, $E_{c;c}$ is the modulus of elasticity in compression of the core and G_c is the shear modulus of elasticity of the core.

As outlined in chapter 2, the total facing compressive stress (in-plane direction) comprises a component due to pure compression and a component due to bending. The total facing compressive stress at the outside of the lower facing is limited by either the characteristic facing compressive strength (Eq. 5) or linear interpolation between the characteristic facing compressive and bending strength dependent on the ratio of stresses due to pure compression and bending (Eq. 6).

$$\sigma_{f,c,tot;x} = \sigma_{f,c,pure;x} + \sigma_{f;m;c;x} = \frac{N}{t_f} + \frac{M_f + \Delta M_f}{W_f} \leq 1 \quad f_{f;c;k} \tag{5}$$

$$\sigma_{f,c,tot;x} = \sigma_{f,c,pure;x} + \sigma_{f;m;c;x} = \frac{N}{t_f} + \frac{M_f + \Delta M_f}{W_f} \leq 2 \quad \text{interpolation } f_{f;c;k} - f_{f;m;k} \tag{6}$$

In Eqs. 5 and 6, N is the in-plane compressive load, t_f is the facing thickness, M_f is the facing bending moment, ΔM_f is the facing bending moment due to second order effects, W_f is facing moment of resistance and x is the in-plane direction (Fig. 7-right).

The core compressive stress is limited by the characteristic core compressive strength.

$$\sigma_{c;c;z} = k\,w \leq f_{c;c} \tag{7}$$

where, w is the displacement of the facing in z-direction and z is the out-of-plane direction (Fig. 7-right).

3.2   Analytical solutions

The limit states outlined in paragraph 3.1.5 are dependent on the in-plane compressive load, the facing bending moment, the facing bending moment due to second order effects and the displacement of the facing in z-direction. A calculation example is given in [9].

The in-plane compressive load N is a direct result of the global mechanical behaviour of the sandwich element. As stated in the introduction, the global mechanical behaviour can be described by the formulas by Berner [4] and De Groot [3], so the in-plane compressive load N can also be described by these formulas.

The facing bending moment M_f, the facing bending moment due to second order effects ΔM_f and the displacement of the facing in z-direction w however, are a direct result of the local mechanical behaviour. The physical linear and geometrical non-linear formulas describing the local mechanical behaviour can be derived by solving the governing differential equation of the mechanical model as illustrated in Figure 7-right. The governing differential equation can be represented by, see Hetenyi [5]:

$$E_{f;m}I_f \frac{d^4w}{dx^4} + N\frac{d^2w}{dx^2} + kw = q \ . \tag{8}$$

If the in-plane compressive load is smaller than the critical load, i.e. $N < 2\sqrt{kE_{f;m}I_f}$, the general solution of the governing differential equation is represented by

$$w(x) = (C_1 e^{\beta_o x} + C_2 e^{-\beta_o x})\cos\alpha_o x + (C_3 e^{\beta_o x} + C_4 e^{-\beta_o x})\sin\alpha_o x + w_o(x) \ , \tag{9}$$

where, $w(x)$ is the displacement of the facing in z-direction (at the interface of the lower facing and the core),

$$\alpha_o = \sqrt{\sqrt{\frac{k}{E_{f;m}I_f}} + \frac{N}{2E_{f;m}I_f}} \ , \qquad \beta_o = \sqrt{\sqrt{\frac{k}{E_{f;m}I_f}} - \frac{N}{2E_{f;m}I_f}} \ , \tag{10}$$

and, $w_o(x)$ is the particular solution of Eq. 8.

The displacement of the facing and the core in z-direction and the facing bending moment will vanish at some distance from the origin, therefore the constants C_1 and C_3 in Eq. 9 have to equal zero. The constants C_2 and C_4 in Eq. 9 can be determined from the condition of

vertical equilibrium at the origin and from the condition of symmetry of the deflected shape at the origin. Both conditions are defined by:

$$-E_{f;m}I_f \frac{d^3w}{dx^3} = \frac{-F}{2} \quad and \quad \frac{dw}{dx} = 0 \,. \tag{11}$$

With these conditions, the displacement of the facing in z-direction $w(x)$ and the facing bending moment including second order effects $M_f(x)$ ($M_f + \Delta M_f$ in Eqs. 5 and 6) can be determined for the case where the out-of-plane load is modelled as one point load (Fig. 8b).

In the case where the out-of-plane load is modelled by two point loads (Fig. 8b), the lower facing is subjected to two point loads, $F/2$ at $x = -L_s/2$ and $x = +L_s/2$, where L_s is the support width. The displacement function of the lower facing in z-direction $w(x)$ and the facing bending moment including second order effects $M_f(x)$ are derived from the analytical solutions derived for the introduction of the out-of-plane load modelled by one point load. This is achieved by adjusting the amplitude and the phase of these analytical solutions. This results in

$$w(x) = \begin{cases} \dfrac{F}{8\sqrt{kE_{f;m}I_f}} \dfrac{e^{-\beta_o L_s/2}}{\alpha_o \beta_o} [\alpha_o f_1(x) + \beta_o f_2(x)] & if \quad 0 \le x \le \dfrac{L_s}{2} \\[3mm] \dfrac{F}{8\sqrt{kE_{f;m}I_f}} \dfrac{e^{-\beta_o x}}{\alpha_o \beta_o} [\alpha_o f_3(x) + \beta_o f_4(x)] & if \quad \dfrac{L_s}{2} \le x \end{cases} \tag{12}$$

$$M_f(x) = \begin{cases} \dfrac{F}{8} \dfrac{e^{-\beta_o L_s/2}}{\alpha_o \beta_o} [\alpha_o f_1(x) - \beta_o f_2(x)] & if \quad 0 \le x \le \dfrac{L_s}{2} \\[3mm] \dfrac{F}{8} \dfrac{e^{-\beta_o x}}{\alpha_o \beta_o} [\alpha_o f_3(x) - \beta_o f_4(x)] & if \quad \dfrac{L_s}{2} \le x \end{cases} \tag{13}$$

where $f_1(x)$ to $f_4(x)$ are given by Eqs. 14 to 17.

$$f_1(x) = e^{-\beta_o x} \cos\alpha_o(x + \frac{L_s}{2}) + e^{\beta_o x} \cos\alpha_o(x - \frac{L_s}{2}) \tag{14}$$

$$f_2(x) = e^{-\beta_o x} \cos\alpha_o(x + \frac{L_s}{2}) - e^{\beta_o x} \sin\alpha_o(x - \frac{L_s}{2}) \tag{15}$$

$$f_3(x) = e^{-\beta_o \frac{L_s}{2}} \cos\alpha_o(x + \frac{L_s}{2}) + e^{\beta_o \frac{L_s}{2}} \cos\alpha_o(x - \frac{L_s}{2}) \tag{16}$$

$$f_4(x) = e^{-\beta_o \frac{L_s}{2}} \cos\alpha_o(x + \frac{L_s}{2}) + e^{\beta_o \frac{L_s}{2}} \sin\alpha_o(x - \frac{L_s}{2}) \tag{17}$$

4   Experimental Analysis

Eight identical full-scale five point bending tests as shown in Figure 9 are carried out to obtain a further understanding of the local mechanical behaviour of structural sandwich elements at an intermediate support. Additionally, the experimental tests are carried out for verification of the limit states and analytical solutions presented in chapter 3. Eight identical experimental tests are carried out to obtain test results that have some statistical relevance.

4.1   Test specimen

This research is limited to the analysis of the local mechanical behaviour at an intermediate support of a two-span structural sandwich roof element type Unidek Kolibrie 3.5 with equal spans of 3000 mm and a width of 300 mm. The material and mechanical properties of chipboard P5 and EPS type 60 are outlined in paragraph 3.1.2 and presented in Table 1 and 2. To obtain conservative test results the externally applied loads on the test specimens are introduced by two point loads at both mid-spans.

4.2   Design of test setup

The test rig is designed in such a way that the test specimen can be installed horizontally and the area around the intermediate support is completely free of rig members (Fig. 9). The undisturbed area around the intermediate support is used to place the measurement setup necessary for ESPI measurements and to accurately monitor the local mechanical behaviour during testing. The design of the test setup requires the rig to be equipped with two relatively large vertical frames and two jacks to be able to introduce two point loads on the test specimen. Great care is taken with respect to the design of the supports and the load introduction in order to capture local failure at the intermediate support. The end supports are designed as roller bearings and the intermediate support is designed as fixed bearing. The latter support comprises a 50 mm wide plywood bearing to ensure local failure at this support. The plywood is equipped with small holes for protection of strain gauges which are applied at the outside of the test specimen. At both load introductions, plywood with a width of 150 mm is used to spread the introduced point loads evenly over the width of the test specimen preventing local failure at these locations. The point loads on the test specimen are applied at a constant displacement of the actuator and the jacks.

cross-section AA'   cross-section BB'

EPS core
lower chipboard
plywood
block steel

detail A1

EPS core
lower chipboard
plywood
block steel

detail A2

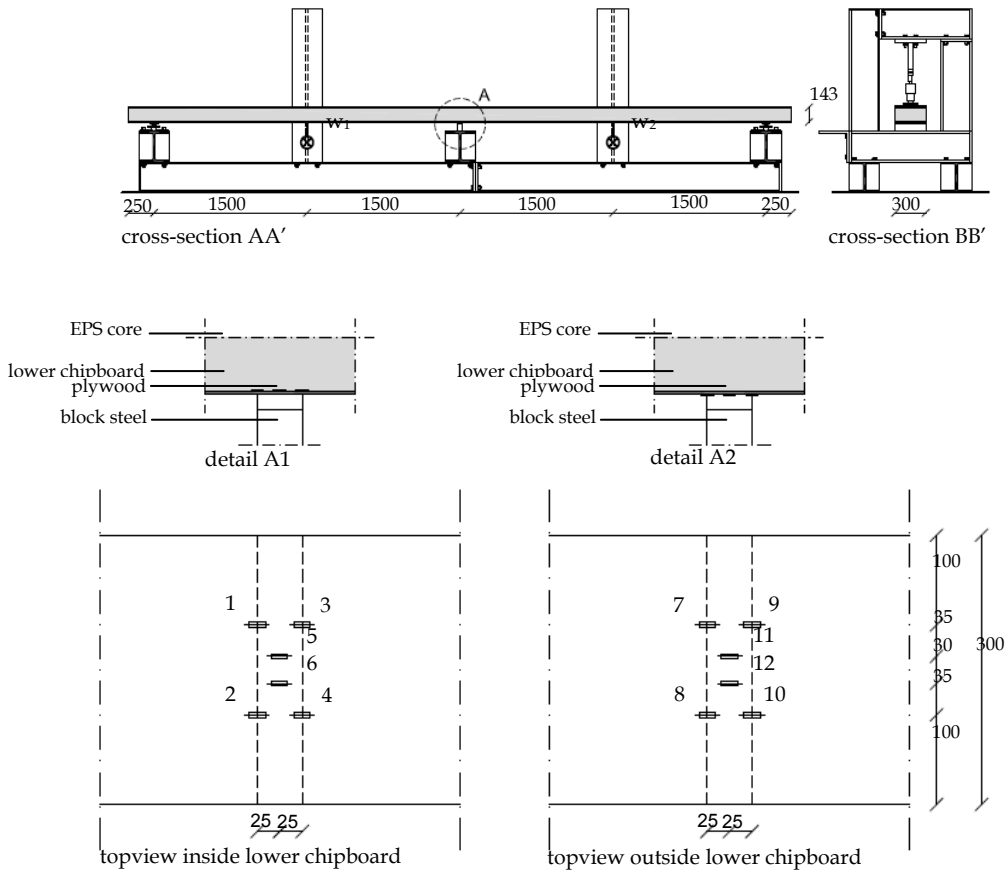topview inside lower chipboard

topview outside lower chipboard

Figure 9. The location of the LVDTs is indicated in cross-section AA' and the locations of the strain gauges are indicated in detail A1 for the inside of the lower chipboard and detail A2 for the outside of the lower chipboard. The numbers refer to the measurement locations. (All dimensions in mm.)

4.3   Measurements

The out-of-plane displacement of the test specimen is measured with LVDTs at the middle of both spans. Furthermore, strains are measured at 12 locations at the intermediate support. The locations of the strain gauges are illustrated in Figure 9, details A1 and A2. On both the inside and the outside of the lower chipboard six strain gauges are placed at exactly the same location. Four strain gauges are located at both the left and right edge of the intermediate support (numbers 1, 2, 7 and 8 (left) and numbers 3, 4, 9 and 10 (right)), as these locations are expected to be loaded by the governing compressive and bending

158

stresses. Four strain gauges are located at the middle of the intermediate support (numbers 5, 6, 11 and 12), to capture the local mechanical behaviour along the width of this support.

4.4 *Experimental results*

In general, all eight full-scale experimental tests have been performed successfully, however unexpected local failure occurred in experimental test A2. In all other experimental tests local failure occurred due to brittle bending tensile failure of the inside of the lower chipboard at the edge of the intermediate support. As outlined in chapter 2, this is the expected governing failure mode. The local mechanical behaviour can be described analytically by limit states Eqs. 5 and 6 (paragraph 3.1.5) and corresponding analytically solution Eq. 13 (paragraph 3.2) by Davies [2]. Experimental test A1 is considered a typical experimental test regarding the global load-displacement behaviour of the test specimen and local load-strain behaviour of the lower facing. Therefore, the results of this experimental test are studied in further detail. This includes that the global load-displacement behaviour is compared to the analytical solution by Berner [4] and De Groot [3] and the local load-stress behaviour, which is derived from the load-strain behaviour, is compared to the aforementioned limit states and analytical solution by Davies [2].

4.4.1 *Global load-displacement behaviour*

The global load-displacement behaviour of experimental test A1 is captured in three parts, as illustrated in Figure 10. The first part (I) starts at the introduction of the loads and ends in point a, the second part (II) starts in point a and ends in point b and the last part (III) starts in point b and ends in point c when global failure at the location of load introduction has been reached. In the first part (I) the test specimen behaves geometrically and physically linear elastic. The second part (II) is characterized by a reducing stiffness, due to physically non-linear behaviour of the lower facing and core. At approximately 1.28 kN per introduced load local brittle bending tensile failure of the inside of the lower facing at the right edge of the intermediate support is initiated. The last part (III) is characterized by a continuation of local failure and finally global failure at the left load introduction. The analytical solution by Berner [4] and De Groot [3] predict the global load-displacement behaviour accurately up to approximately 1.0 kN per introduced load. From that point the analytical solution overestimates the stiffness of the test specimen due to physical non-linear behaviour of both the lower facing and core which is not taken into account by the analytical solution.
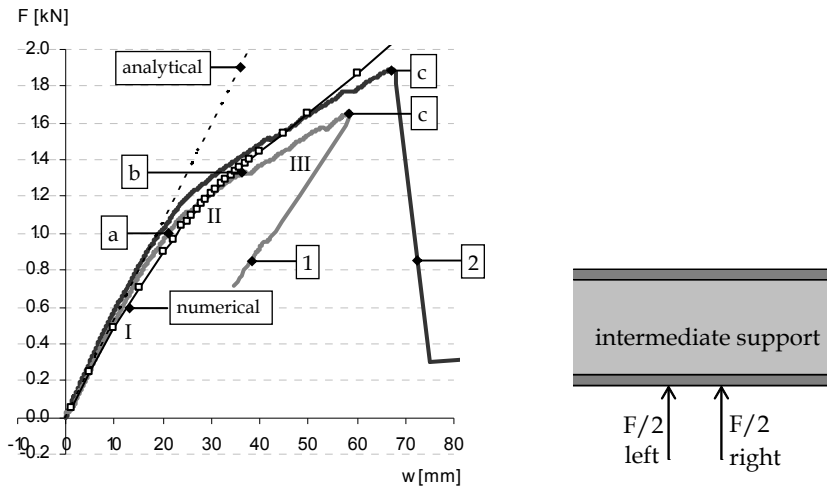
Figure 10. Load-displacement graphs of experimental test A1 (black and grey lines), analytical solution by Berner [4] and De Groot [3] (dotted line) and numerical analysis (black line with small boxes). The numbers refer to the measurement locations indicated in Figure 9. The Roman numbers refer to the different parts of the load-displacement graphs and the letters refer to specific points on the load-displacement graphs.

4.4.2 Local load-strain and load-stress behaviour

Figure 11 shows the local load-strain behaviour at the edges of the intermediate support. It can be seen that the load-strain behaviour is geometrically and physically non-linear as all load-strain graphs are curved. Up to approximately 1.0 kN per introduced load, this curvature is caused by geometrical non-linear behaviour as the load-displacement graphs in Figure 10 show physically linear elastic behaviour of the test specimen up to this load. From approximately 1.0 kN per introduced load, this curvature is caused by the combined effects of geometrical and physical non-linear behaviour. Figure 11 shows that the outside of the lower facing is subjected to compression and the inside of the lower facing is first subjected to compression and then subjected to tension. At approximately 1.28 kN per introduced load, local brittle bending tensile failure is initiated at the right edge of the intermediate support (point b in Figure 10). This failure load corresponds to a strain of approximately 0,0075 mm/mm equivalent to a stress of 27.8 N/mm² (assuming Hook's law is valid). This value exceeds the characteristic bending strength of 16.06 N/mm² (Table 1) probably due to biaxial stresses in the lower facing resulting in a higher characteristic bending strength, a higher bending strength of the lower facing compared to the

160

characteristic bending strength, inwards directed local failure or initiation of local failure before it is detected by the strain gauges resulting in unrealistically high measured strains and thus stresses.
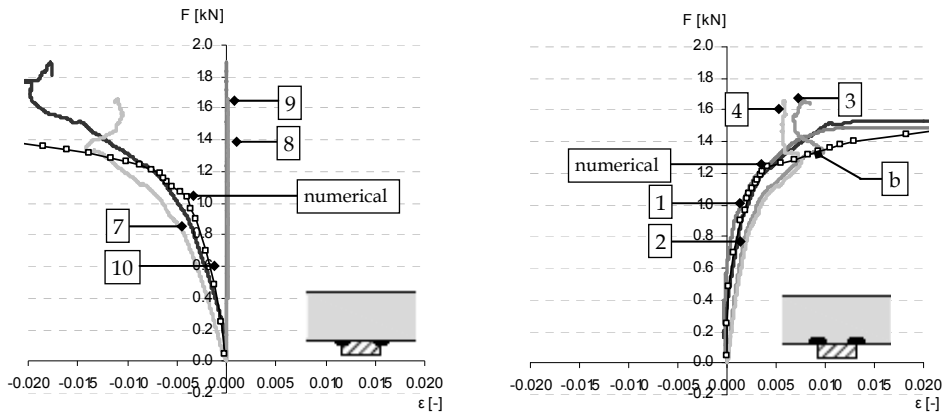

Figure 11. Load-strain graphs for the outside and the inside of the chipboard at the edges of the intermediate support obtained from experimental test A1 (black and grey lines) and numerical analysis (black line with small boxes). The numbers refer to the measurement locations indicated in Figure 9. The letter b indicates local brittle bending tensile failure at the right edge of the intermediate support.
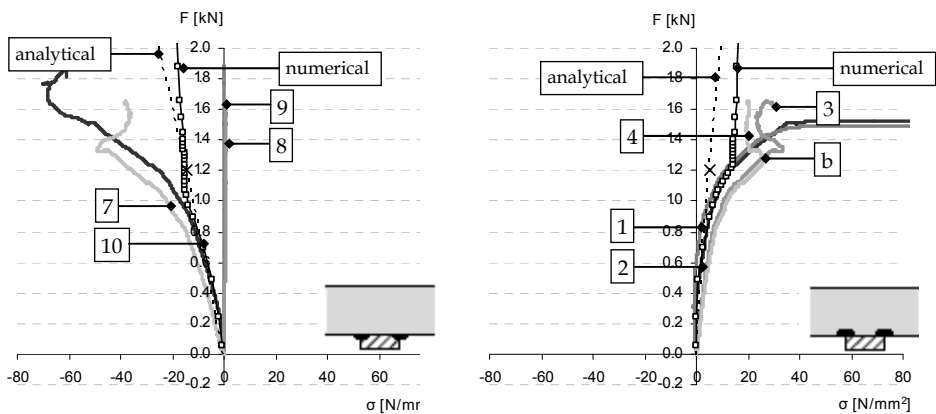

Figure 12. Load-stress graphs for the outside and the inside of the chipboard at the edges of the intermediate support obtained from experimental test A1 (black and grey lines), the limit state (Eq. 5) and corresponding analytical solution (Eq. 13) by Davies [2] for situation 1 (dotted line) and numerical analysis (black line with small boxes). The maximum load capacity as defined by Davies [2] is marked by a cross. The numbers refer to the measurement locations indicated in Figure 9. The letter b indicates local brittle bending tensile failure at the right edge of the intermediate support.

Figure 12 shows the load-stress behaviour at the edges of the intermediate support. The stresses are derived from the measured strains by applying Hook's law. This law is only valid for physical linear elastic material behaviour. Therefore, the load-stress graphs (in compression) are only valid up to the point where the characteristic compressive strength of the lower facing is reached. The load-strain graphs show no clear transition between physical linear elastic behaviour and physical non-linear behaviour at the outside of the lower facing. Therefore, the point where the characteristic compressive strength of the outside of the lower facing is reached, thus the point up to where the load-stress graphs are valid, is difficult to indicate. However, this point is reached at some point after 1.0 kN per introduced load as the load-displacement graphs in Figure 10 show physically linear elastic behaviour of the test specimen up to approximately 1.0 kN per introduced load.

The load-stress behaviour can be compared to the limit states and corresponding analytical solutions by Davies [2]. It can be seen that the analytical results predict the load-stress behaviour accurately up to approximately 0.9 kN. From this point the experimental results start to diverge from the analytical results. This may be explained by the fact that the analytical results are only valid for small rotations however the experimental tests show that the effects of large rotations may not be neglected. The analytical results therefore underestimate the effects of the local bending moment in the lower facing resulting in less pronounced geometrical non-linear behaviour. Another explanation for the divergence of the experimental results can be found in the negligence of physical non-linear behaviour of both the lower facing and core by the analytical results, however the experimental tests show physical non-linear behaviour of the core from approximately 1.0 kN and physical non-linear behaviour of the facing at some point after approximately 1.0 kN. The analytical results therefore overestimate the stiffness of the test specimen resulting in inaccurate load-stress behaviour from approximately 1.0 kN.

The measured ultimate loads off all experimental tests are shown in Table 3. The ultimate loads predicted by the limit states (Eqs. 5 and 6) and corresponding analytical solutions by Davies [2] are also shown for two situations:

1. Limit state defined as the characteristic compressive strength, resulting in an average ultimate load of 1,20 kN per introduced load.
2. Limit state defined as the interpolation between the characteristic compressive and bending strength, resulting in an average ultimate load of 1.28 kN per introduced load.

162

Table 3. Ultimate load (per introduced load) measured for all experimental tests and predicted by limit states and corresponding analytical solution by Davies [2] (All loads in kN.)

Test specimen	A1	A2	A3	A4	B1	B2	B3	B4	Average
Experimental results	1.28	1.16	1.36	1.40	1.54	1.46	1.39	1.48	**1.38**
Results by Davies [2]									
1. $f_{f;c;k}$ * (Eq. 5)	1.21	1.22	1.18	1.17	1.23	1.17	1.19	1.22	**1.20**
2. $f_{f;c;k} - f_{f;m;k}$ ** (Eq. 6)	1.30	1.31	1.26	1.25	1.32	1.25	1.27	1.30	**1.28**

* Limit state of the core as presented in Eq. 7 is reached or slightly exceeded for all experimental tests.
** Limit state of the core as presented in Eq. 7 is considerably exceeded for all experimental tests.

The average measured ultimate load equal to 1.38 kN per introduced load is 15% higher than 1.20 kN and 8% higher than 1.28 kN.

Remark: the characteristic core compressive strength is reached or slightly exceeded for situation 1 and considerably exceeded for situation 2 for all analytically predicted ultimate loads. Therefore, situation 2 does not predict a reliable ultimate failure load and the ultimate failure load of situation 1 is adopted in this research.

4.5   *Main conclusions*

Based on the experimental analysis the following main conclusions can be drawn.

- The experimental results strongly indicate that structural sandwich elements become sensitive to early local brittle bending tensile failure at the intermediate support if the width of this support is relatively small. All experimental results namely showed early local brittle bending tensile failure at the intermediate support before global tensile failure at mid-span or at the intermediate support could occur (the experimental tests are properly designed to obtain this failure mechanism). Since the width of the intermediate support equals the girder width, about 50-70mm, this failure mechanism cannot be ignored.

- The experimental results strongly indicate that the analytically predicted local behaviour and failure mechanism of structural sandwich elements at the edges of the intermediate support is correct. The test results of the stain gauges namely showed that the outside of the lower chipboard was subjected to only compression and the inside of the lower chipboard was first subjected to compression and then to tension before local brittle bending tensile failure was initiated. This indicates that the stresses in the lower chipboard comprise a component due to pure compression and bending and failure is initiated by exceeding the characteristic bending strength.

Consequently, the introduction of the out-of-plane load as two point loads, two times F/2 as indicated in Figure 8b, seems to be correct.

- The experimental results strongly indicate that the limit states and corresponding analytical solutions by Davies [2] underestimate the local geometrical non-linear behaviour as they are only valid for second order linear elastic behaviour. Furthermore, the experimental results strongly indicate that the limit states and corresponding analytical solutions by Davies [2] overestimate the stiffness of the structural sandwich element at the intermediate support as they do not take into account the physical non-linear behaviour of both the facing and core.

- The experimental results strongly indicate to assume that the limit states and corresponding analytical solutions by Davies [2] predict a conservative ultimate failure load as the difference between the measured ultimate load and the average analytically predicted ultimate load, assuming the compression strength of the chipboard is the limiting factor (situation 1), is about 15%.

5   Numerical Analysis

A numerical model is developed to obtain a further understanding of the local mechanical behaviour of structural sandwich elements at an intermediate support. Additionally, numerical simulations are performed for verification of the limit states and analytical solutions presented in chapter 3.

5.1   Numerical model

Although particular attention is given to develop a numerical model representing the rather complex local mechanical behaviour at an intermediate support of structural sandwich elements, some simplifications are made as not all parameters could or have been measured. Simplifications are made to the out-of-plane straightness of the sandwich element, the adhesive layer at the interface of the facings and core and the mechanical properties of the facing and core material. Furthermore, the end supports and the load introduction are idealized, however the intermediate support was modelled in more detail to ensure accurate numerical results.

The nominal values of the sandwich element are adopted in the numerical model as a maximum deviation of the measured dimensions of all test specimens is less than 5%. The out-of-straightness of two out of eight test specimens is not modelled as the experimental results are corrected for the inaccuracies caused by the out-of-straightness.

5.1.1 Modelling the chipboard facings

The chipboard facings are modelled by PLANE82 elements as these elements are commonly used to represent two-dimensional plane stress problems. A reduced 2x2 Gauss numerical integration scheme is adopted for the integration of the stiffness and stress stiffness matrices.

The orthotropic material properties of chipboard (Table 1), which are adopted from literature Blaß et al [6], EOTA [7], De Groot [3], are specified for the PLANE82 elements. However, the different behaviour of chipboard in compression, tension and bending cannot be applied as this behaviour cannot be described by the available material models. Therefore, the mechanical properties of chipboard in compression, tension or bending are applied at those locations were the chipboard is mainly subjected to respectively compression, tension or bending. The full-scale experimental tests show that the chipboard material is loaded beyond the elastic range at the location of the intermediate support. Therefore, an idealized bi-linear stress-strain diagram based on the mechanical properties of chipboard in compression as shown in Figure 13 is used to represent the material behaviour in compression and bending. The idealized stress-strain diagram does not predict brittle bending tensile failure. Therefore brittle bending tensile failure of the inside of the lower chipboard is simulated when the characteristic compressive strength is reached.
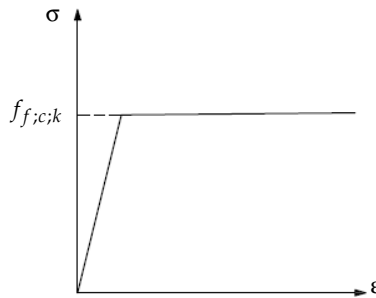

Figure 13. Idealized stress-strain diagram adopted for the material behaviour of chipboard in compression

5.1.2 Modelling the EPS core and intermediate support

The EPS core is modelled by the same PLANE82 elements as used for the chipboard facings. The material properties of EPS (Table 2), which are adopted from literature EOTA [7], De Groot [3], are specified for the PLANE82 elements.

At the intermediate support the stress-strain relation of the EPS material is represented by a multi-linear stress-strain diagram (Fig. 14), based on results of compressive tests performed by Kingspan - Unidek B.V.. At other locations, the EPS material is loaded within the elastic range. Therefore, it is considered sufficient to model the EPS material behaviour as linear elastic at other locations. Modelling of physical non-linear material behaviour of the EPS material at the load introduction is not taken into account, as in the experimental analysis the load introduction is designed such that the loads are spread sufficiently into the EPS material. Modelling of residual stresses originated in the production process is not taken into account.
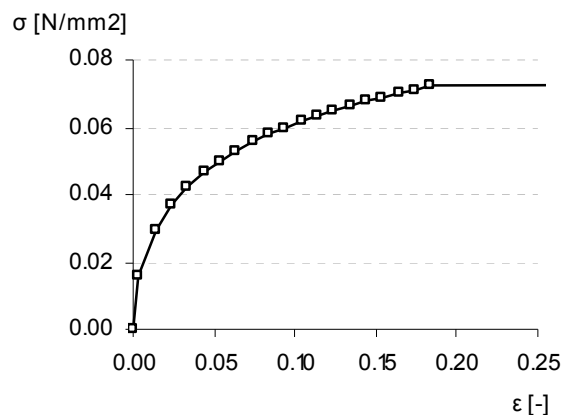

Figure 14. Multi-linear stress-strain diagram adopted for the material behaviour of EPS at the location of the intermediate support

The plywood intermediate support is modelled by the same PLANE82 elements as used for the chipboard facings. The orthotropic material properties of plywood, which are adopted from literature Blaß *et al*. [6], are specified for the PLANE82 elements and a linear elastic stress-strain relation is modelled.

5.1.3 Modelling the boundary conditions

To accurately simulate the local mechanical behaviour at the intermediate support, the geometry of the sandwich element is connected to the geometry of the intermediate support by modelling an interface layer that comprises a flexible contact between two associated element types, TARGE169 and CONTA172. The pure Lagrange multiplier method is applied as contact algorithm as this method enforces zero penetration within certain tolerances when contact is closed.

By using symmetry conditions only half the sandwich structure has to be modelled resulting in an efficient model and a reduction of computational time. The end supports of the sandwich model are idealized as simple roller supports and to prevent rigid body motion the geometry of the intermediate support is hinged supported. The numerical model consists of a fine mesh near the intermediate support, a transition zone and a coarse mesh. Local mesh refinement at the intermediate support is applied to obtain accurate results.

5.1.4 Solution procedure

All numerical analyses in this research are performed with the Finite Element program ANSYS 11.0 as displacement controlled geometrical and physical non-linear analyses in which the Newton-Raphson step-by-step incremental iterative solution procedure is adopted.

5.1.5 Calibration Finite Element model

The calibration of the Finite Element model is based on the results obtained from the experimental tests, the mechanical properties adopted from literature Blaß et al [6], EOTA [7] and De Groot [3] and the assumed stress-strain relation of the EPS core based on results of compressive tests performed by Kingspan - Unidek B.V.

5.2 Numerical results and main conclusions

The discussion of the results obtained from the numerical analysis focuses on the global load-displacement behaviour and the local mechanical behaviour. For the global load-displacement behaviour, the numerical results are compared to the analytical solution by Berner [4] and De Groot [3] and the test results of experimental test A1 (Fig. 10). For the local mechanical behaviour, the numerical results are compared to the limit state and corresponding analytical solution by Davies [2] and the test results of experimental test A1 (Fig. 11 and Fig. 12). Based on the comparison of the numerical, analytical and experimental results the following main conclusions can be drawn.

- The results obtained from the numerical analysis predict the global load-displacement behaviour and local mechanical behaviour quite well. The load-displacement graphs obtained from the numerical analysis and experimental test A1 capture similar load-displacement behaviour and the absolute and relative differences are small. The load-strain and load-stress graphs obtained from the

numerical analysis and experimental test A1 show similar local mechanical behaviour at the edges of the intermediate support and local failure is found at the inside of the lower facing at the edge of the intermediate support.

- The load-strain graphs obtained from the numerical analysis show no unloading at initiation of local brittle bending tensile failure of the inside of the lower facing at the edge of the intermediate support. The numerical model cannot simulate brittle bending tensile failure and thus unloading as the stress-strain relation modelled for chipboard in bending is based on chipboard in compression. Consequently, the inside of the lower facing shows physical non-linear behaviour instead of brittle bending tensile failure.

- The load-stress graphs obtained from the numerical analysis correspond to the load-stress graphs obtained from the analytical analysis up to a load of 1.0 kN per introduced load. From this load, the analytical results start to diverge from the numerical results. This can be explained, as discussed before, by the fact that the analytical results are only valid for small rotations and do not take into account physical non-linear behaviour of both the lower facing and core.

- The numerical and experimental results strongly indicate that the limit state and corresponding analytical solution by Davies [2] predict a conservative failure load. The numerically and experimentally obtained average ultimate load equal to 1.24 kN and 1.38 kN per introduced load are respectively 3.3% and 15.0% higher than the average analytically obtained ultimate load equal to 1.20 kN per introduced load.

Remark: In [9], the analytical solution presented by the SKH publication [1] is discussed. The numerical and experimental results strongly indicate that this analytical solution predicts a conservative failure load. The numerically and experimentally obtained average ultimate load are respectively 118% and 142% higher than the analytically obtained ultimate load equal to 0.57 kN per introduced load. This can be explained by the fact that the analytical solution overestimates the local bending moment in the lower facing as the load introduction at the intermediate support is represented by one point load (Fig. 8b).

6 Conclusions

Based on the analytically, experimentally and numerically obtained results it can be concluded that structural sandwich elements can become sensitive to early local failure. In this case, the load-bearing capacity of structural sandwich elements is limited by local brittle bending tensile failure of the inside of the lower chipboard at the edge of the intermediate support due to a combination of an in-plane compressive load and an out-of-plane load. Since the relatively small adopted width of 50 mm in this research is equal to the generally applied girder width of about 50-70 mm, it is concluded that this local failure mechanism cannot be ignored.

In publications by SKH [1] and Davies [2] univocal local mechanical behaviour and failure of structural sandwich elements at an intermediate support is described, but both publications are not univocal regarding the derivation and formulation of the analytical solutions. Based on this research, it can be concluded that the existing analytical solutions by SKH [1] and Davies [2] both predict a safe ultimate load. The assumption of unsafe existing analytical solutions concerning the local mechanical behaviour concluded by De Groot [3] is partly based on an incorrect application of these existing analytical solutions and thus incorrect calculated ultimate loads.

The limit state for the lower facing based on the compressive strength (situation 1, Eq. 5) and corresponding analytical solution based on a load introduction as two times F/2 as indicated in Figure 8b (Eq. 13) (Davies [2]), describe the local mechanical behaviour at an intermediate support of a structural sandwich element most accurate and predict a safe ultimate load. In the analytical solution a modified foundation constant (Eq. 2) is adopted.

Finally, the research objective is fulfilled as the aforementioned limit state and corresponding analytical solution can be regarded as an improved and reliable analytical design approach for the local mechanical behaviour of structural sandwich elements at an intermediate support. This design approach is proposed to be used in practice.

Literature

[1] Stichting Keuringsbureau Hout, SKH Publicatie 92-02, Houtachtige dakconstructies: rekenprogramma voor sandwichelementen en enkelhuidige ribpanelen, 1994, SKH, Huizen.

[2] J.M. Davies, *Lightweight sandwich construction*. 2001, MPG Books Ltd, Cornwall.

[3] W.H. de Groot, Buigings- en dwarskracht vervorming van sandwichpanelen, "Ontwikkelen van een eenvoudig toepasbare rekenmethode voor statisch onbepaalde sandwichconstructies, vergeleken met laboratoriumexperimenten." 2008, Technische Universiteit Eindhoven, Eindhoven.

[4] H. Berner, Praxisgerechte nachweise zur trag- und gebrauchsfähigkeit von sandwichbauteilen. 1998, *Stahlau*, 67 pp. 910-925.

[5] M. Hetenyi, *Beams on elastic foundation: theory with applications in the fields of civil and mechanical engineering*, 1958, 5th edn, University of Michigan press, S.I.

[6] H.J. Blaß, J. Elhbeck, H. Kreuzinger and G. Steck, Entwurf, Berechnung und Bemessung von Holtzbauwerken. Algemeine Bemessungsregeln und Bemessungsregeln für den Hochbau,(BEKS). 2004, DGfH Innovation und Service GmbH, München.

[7] EOTA. Technical report 019, Calculation models for prefabricated wood-based loadbearing stressed skin panels for use in roofs, 2005, European Organisation for Technical Approvals, Brussel.

[8] H.G. Allen, *Analysis and design of structural sandwich panels*, 1969, Pergamon Press, Oxford.

[9] R.A. Luimes, Local behaviour of structural sandwich elements at an intermediate support, 2011, University of Technology Eindhoven, Eindhoven.

[10] Kingspan - Unidek B.V.